JOURNAL OF SOLID STATE CHEMISTRY 74, 138–146 (1988)

The Vibrational Spectra of the Layered Compounds $K_3Sb_3M_2O_{14},xH_2O$ (M = P, As): Normal Coordinate Analysis of $K_3Sb_3P_2O_{14},xH_2O$

E. HUSSON*

Laboratoire de Chimie Physique du Solide, UA CNRS 453, Ecole Centrale des Arts et Manufactures, 92295 Chatenay-Malabry Cedex, France

AND A. LACHGAR AND Y. PIFFARD

Laboratoire de Chimie des Solides, UA CNRS 279, 2, Rue de la Houssinière, 44072 Nantes Cedex 03, France

Received September 23, 1987; in revised form December 3, 1987

Infrared and Raman spectra on powder samples of $K_3Sb_3P_2O_{14},xH_2O$ and $K_3Sb_3As_2O_{14},xH_2O$ and polarized Raman spectra on a single crystal of $K_3Sb_3P_2O_{14},xH_2O$ have been recorded. A normal coordinate analysis using a generalized valence force field has been performed. All the normal modes of vibration are described in terms of potential energy distribution. The validity of the force field and the values of the force constants are discussed. © 1988 Academic Press, Inc.

Introduction

The isostructural compounds $K_3Sb_3M_2O_{14},xH_2O$ (M = P, As) are layered materials (*1, 2*) and can be easily ion exchanged in acidic medium thus leading to the corresponding phosphato- and arsenoantimonic acids. These latter compounds are very good ion exchangers (*3*) and protonic conductors (*4*) and are also studied for their catalytic properties. In this paper, the infrared and Raman spectra of both compounds are compared. Then a normal coordinate analysis (NCA) carried out for the phosphatoantimonate permits us to make precise band assignments for the vibrational modes and to obtain information about the chemical bonds from the calculated force constants.

Experimental

$K_3Sb_3M_2O_{14},xH_2O$ compounds have been prepared as described previously (*1, 2*). The bulk of the crystals obtained are hexagonal-shaped platelets with large (001) faces of about 0.5 mm maximum dimension.

The infrared absorption spectra were recorded in the range 4000–200 cm^{-1} with a Philips-Pye Unicam PU 9512 spectrophotometer equipped with a purging device to maintain a moisture- and CO_2-free atmosphere in the instrument. These spectra were obtained using CsI pellets technique. The absorption bands were reproducible to ± 2 cm^{-1}.

The Raman spectra of powder samples were recorded with a CODERG T800 spectrometer; scattered radiation was collected at 90° to the direction of the incident beam.

* To whom correspondence should be addressed.

0022-4596/88 $3.00

For the polarized spectra, a Microdil 28 equipment with a retrodiffusion geometry was used. Both spectrometers were equipped with an argon ion laser as an excitation source (λ = 514.5 nm).

The NCA treatment of $K_3Sb_3P_2O_{14},xH_2O$ was done with Schachtschneider's programs (*5*) modified by Bates (*6*) according to Shimanouchi's method (*7*) and a generalized valence force field was chosen. The average difference between the assigned observed and calculated frequencies is about 2.2%.

Results and Discussion

Previous Structural Data

The layered compounds $K_3Sb_3M_2O_{14},xH_2O$ (M = P, As) crystallize in the rhombohedral system, space group $R\bar{3}m$ with a = 7.147(1) Å and c = 30.936(6) Å when M = P and a = 7.232(2) Å and c = 31.606(5) Å when M = As, Z = 3. They are isomorphous. The crystal structure of the phosphorus phase was determined from X-ray diffraction data (*1*).

The $(Sb_3P_2O_{14}^{3-})_n$ layers are built up from SbO_6 octahedra and PO_4 tetrahedra sharing corners (Fig. 1). In the (001) plane the SbO_6 octahedra are linked together exactly in the same way as the WO_6 octahedra in the (001) plane of the hexagonal tungsten bronze. The PO_4 tetrahedra are linked to these layers of octahedra on both sides, via three of their vertices and the fourth, which is unshared, points into the interlayer space. The potassium atoms and water molecules are statistically distributed over different sites in the interlayer space. They are not bonded very tightly to the $(Sb_3P_2O_{14}^{3-})_n$ covalent layers. Indeed the potassium atoms can be easily ion exchanged and when heated up to 180°C the compound becomes anhydrous. In this structure, there are two types of Sb–O bonds:

—The d_1 bonds (1.944(1) Å) are close to the layer plane. Their oxygen atom is shared with another antimony atom and one potassium atom (K–O = 2.748(5) Å).

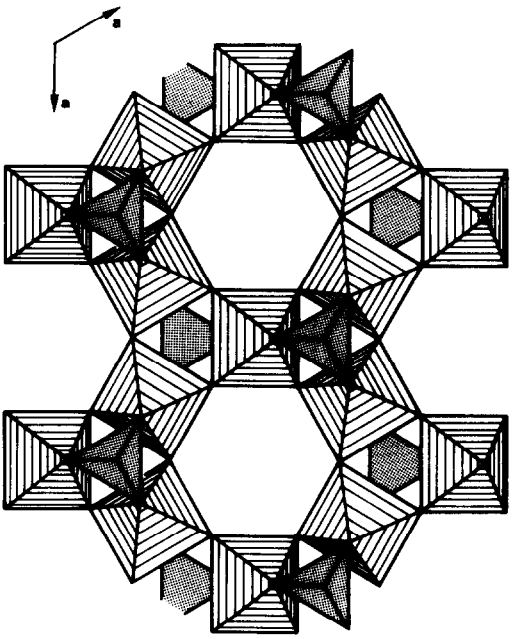

FIG. 1. Projection along the c axis of a $(Sb_3P_2O_{14}^{3-})_n$ layer.

—The d_2 bonds (2.014(3) Å) are nearly perpendicular to the layers. Their oxygen atom is shared with a phosphorous one and one potassium atom (K–O = 2.947(2) Å).

There are also two types of P–O bonds:

—The D_1 bonds (1.486(6) Å) for which the oxygen atom, considered as unshared, points into the interlayer space;

—The D_2 bonds (1.563(2) Å) for which the oxygen atom is also bonded to antimony.

For the K–O bonds, taking into account the ionic radii of potassium and oxygen (*8*), only those with a length less than 3 Å are considered to play a significant role in the structure.

Theoretical Numbering of Vibrations

For the numbering of vibrations by the method of Bhagavantam and Venkataryudu

(*9*) it is necessary to account for the symmetry and then to consider the potassium sites as fully occupied. The factor group analysis carried out at $\mathbf{k} = 0$ gives:

$$\Gamma_{\text{optic modes}} = \underset{(R)}{24A_{1g}} + \underset{(i)}{6A_{2g}} + \underset{(R)}{30E_g} + \underset{(i)}{9A_{1u}} + \underset{(ir)}{29A_{2u}} + \underset{(ir)}{38E_u}$$

$$\Gamma_{\text{acoustic modes}} = A_{2u} + E_u,$$

where R stands for Raman active, ir for infrared active, and i for inactive. In $K_3Sb_3P_2O_{14},xH_2O$ the bonds within the layers are strong and mainly covalent while those between adjacent layers are weak, essentially K–O bonds, hydrogen bonds, and van der Waals. Consequently adjacent layers do not interact very much. Furthermore, if one assumes that the layers vibrate in phase it is then possible to simplify the elementary unit cell by considering only one layer instead of three and to classify the crystal modes as follows:

$$\Gamma_{\text{op}(Sb_3P_2O_{14}^{3-})_n} = 6A_{1g} + 2A_{2g} + 8E_g + 3A_{1u} + 7A_{2u} + 10E_u$$

$$\Gamma_{\text{op}(K^+)} = 2A_{1g} + 2E_g + 2A_{2u} + 2E_u$$

$$\Gamma_{\text{ac}} = A_{2u} + E_u$$

Eighteen Raman lines and 21 infrared bands are then predicted; the frequencies due to K–O bonds are expected in the very low frequency region ($\leq$150 cm^{-1}).

Halford's method (*10*) can be applied to the analysis of the internal modes of the PO_4 groups. The tetrahedral PO_4^{3-} ion with T_d symmetry has four internal modes of vibration, i.e., (ν_1) 938 cm^{-1}, (ν_2) 420 cm^{-1}, (ν_3) 1017 cm^{-1}, (ν_4) 567 cm^{-1} (*11*). Table I gives the correlation diagram between the PO_4^{3-} free group vibrations in the T_d symmetry and the PO_4^{3-} lattice internal vibrations in the D_{3d} symmetry via the C_{3v} symmetry of one PO_4 in the crystal. It is seen that, for the antisymmetric P–O stretching, two modes are predicted both in Raman and ir spectra and, for the symmetric stretching, one mode is predicted in Raman and ir spectra.

TABLE I

CORRELATION DIAGRAM FOR PO_4 GROUPS

	T_d ideal symmetry		C_{3v} real symmetry site symmetry	D_{3d} factor group	Assignment
(1017)[a]	ν_{as}	F_2	A_1	A_{1g}	1211
				A_{2u}	1284–1255
			E	E_g	1095
				E_u	1190
(938)	ν_s	A_1	A_1	A_{1g}	984
				A_{2u}	970–955
(567)	δ_1	F_2	A_1	A_{1g}	
				A_{2u}	
			E	E_g	
				E_u	
(420)	δ_2	E	E	E_g	
				E_u	

[a] For a free PO_4^{3-} ion of T_d symmetry (after (*11*)).

Vibrational Spectra Analysis

The powder Raman and ir spectra of the two compounds are illustrated in Figs. 2 and 3. It can be pointed out that the total number of observed frequencies is close to the number predicted with a simplified unit cell. The 1300- to 900-cm^{-1} domain in Figs. 2a and 3a and 1020- to 840-cm^{-1} domain in Figs. 2b and 3b can be assigned, respectively, to P–O and As–O stretching vibrations. In the low frequency region, both compounds have three ranges in common on their spectra:

—ranges 790–700 and 550–400 cm^{-1} can be assigned to d_1 and d_2 stretching modes;

—range 400–200 cm^{-1} can be assigned to O–Sb–O bending modes.

Polarized Raman spectra were recorded for different orientations of the crystal. The $y(\ )\bar{y}$ spectra are represented in Fig. 4 where the polarization conditions are given using the notation of Porto and Scott (*12*). Six A_{1g} lines are observed in Fig. 4a for the covalent skeleton and only one line for the

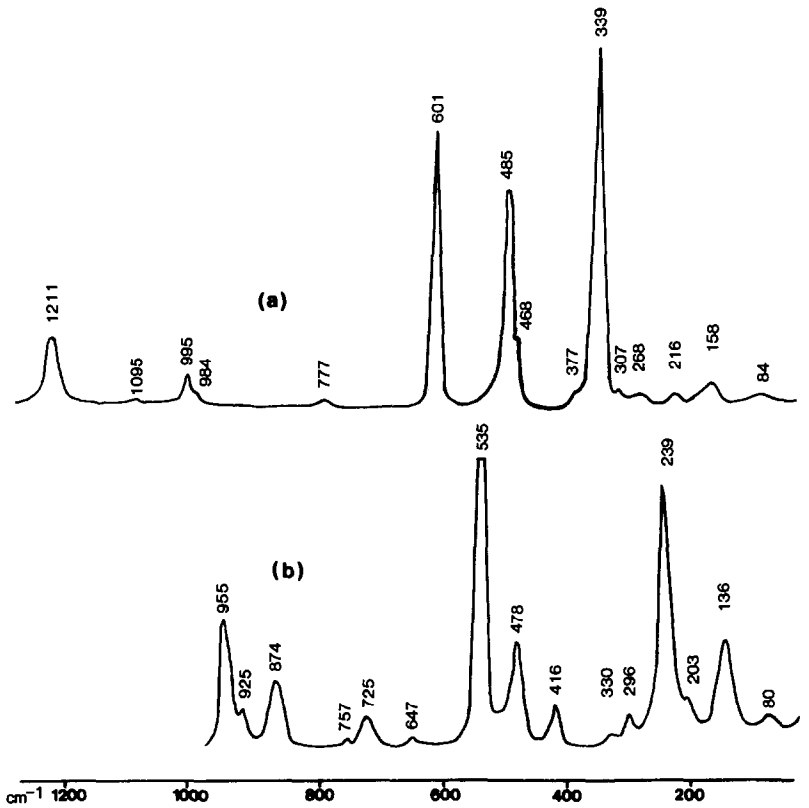

FIG. 2. Raman spectra of (a) $K_3Sb_3P_2O_{14},xH_2O$ and (b) $K_3Sb_3As_2O_{14},xH_2O$.

K–O bonds instead of two. For the E_g modes, eight lines are expected for the covalent skeleton and two lines in the low frequency region. Eight lines are observed unambiguously in the high frequency region plus two possible lines at 995 and 599 cm^{-1} and no line for the low frequency region (Fig. 4b). Figure 4c confirms the assignment and shows two distinct lines at 995 and 984 cm^{-1}. However, if one considers the correlation diagram of Table I, it becomes possible to assign the frequencies due to the P–O stretching modes. In the Raman spectra the A_{1g} modes at 1211 and 984 cm^{-1} are respectively assigned to a ν_{as} and a ν_s mode, the 1095 cm^{-1} E_g mode to a ν_{as} mode. So the 995 cm^{-1} line cannot be assigned. Its value, very close to the 984-cm^{-1} A_{1g} line, seems to indicate that it corresponds to a splitting of this line due to the interlayer interactions so far supposed as negligible in the calculations, or to the presence of some water molecules in the interlayer space (see below). The same feature is observed in the ir spectra where the two bands at 970 and 955 cm^{-1} correspond to the A_{2u} ν_s stretching mode. The ir bands at 1284–1255 and 1190 cm^{-1} are assigned, respectively, to the A_{2u} and E_u ν_{as} modes.

For ionic phosphates, the bands assigned to a ν_s mode in a PO_4^{3-} group are generally stronger in the Raman spectra than the bands assigned to a ν_{as} mode and conversely in the infrared spectra. This is not the case here, but, one must observe first that the PO_4 tetrahedra in $K_3Sb_3P_2O_{14},nH_2O$ are part of a strongly covalent network and then that the four P–O bonds are not equiv-

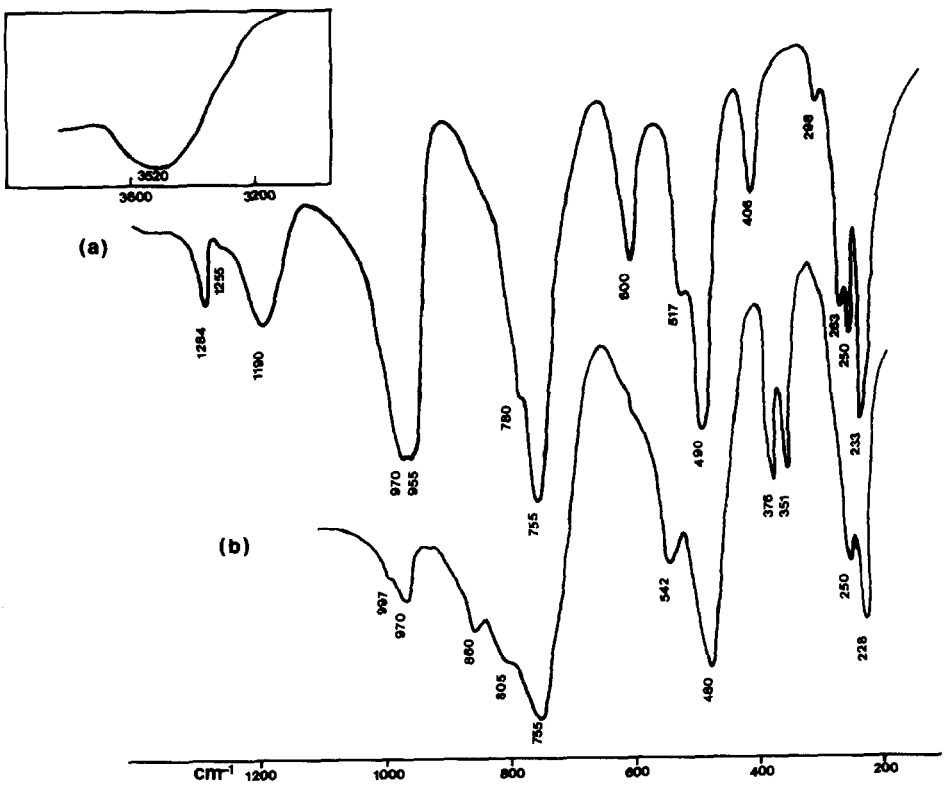

FIG. 3. Infrared absorption spectra of (a) $K_3Sb_3P_2O_{14}, xH_2O$ and (b) $K_3Sb_3As_2O_{14}, xH_2O$.

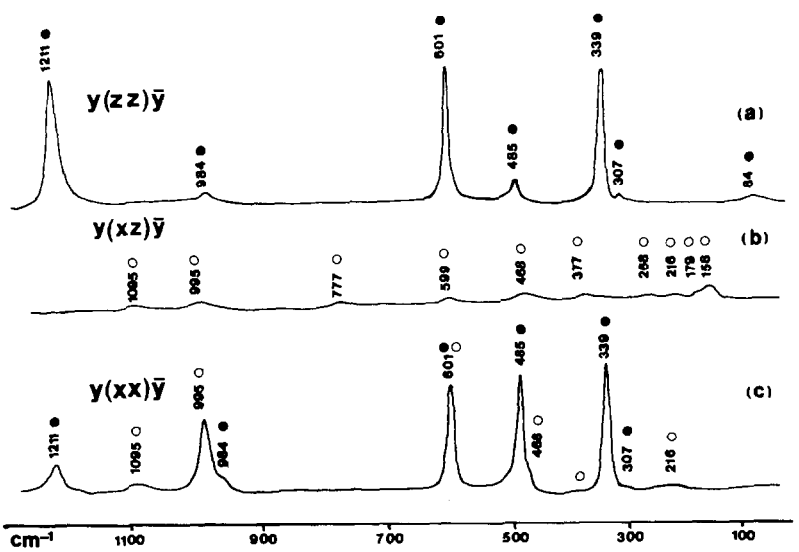

FIG. 4. Polarized Raman spectra of $K_3Sb_3P_2O_{14}, xH_2O$.

alent; the P–O terminal bond is much stronger than the other three.

NCA Treatment

For the NCA treatment, all the stretching and bending coordinates for the covalent framework $(Sb_3P_2O_{14}^{3-})_n$ and only one set of K–O bonds, the shortest in the structure (2.75 Å), have been introduced. A torsion coordinate around d_1 bonds has also been considered. The sets of internal coordinates chosen are given in Table II. Thirty-five atoms (Fig. 5) were needed to define 104 internal coordinates and 65 symmetry coordinates which were reported elsewhere (*13*). In order to obtain a better fit between the observed and calculated frequencies, eight stretching/stretching interactions were also incorporated; they are defined in Table II.

TABLE II

DEFINITION AND CALCULATED FORCE CONSTANTS FOR $K_3Sb_3P_2O_{14},xH_2O$

Definition		Concerned atoms (Fig. 5)	f^a
Sb–O	d_1	1–4	2.97
	d_2	1–10	2.60
O–Sb–O	γ_1	4–1–9	0.63
	γ_2	4–1–29	
	γ_3	4–1–10	0.78
	γ_4	10–1–29	
P–O	D_1	21–17	8.50
	D_2	21–10	6.62
O–P–O	β_1	10–21–12	0.90
	β_2	10–21–17	
P–O–Sb	δ	21–10–1	0.72
Sb–O–Sb	α	1–4–3	0.00
O–Sb–O–Sb	τ	(29, 9, 10, 14)–1–4–3	0.00
K–O	Δ	18–19	0.30
Sb–O/Sb–O	d^*	4–1/1–29	0.15
	d^0	1–4/4–3	0.05
	d_1'	10–1/10–21	0.27
P–O/Sb–O	d_2D_2	1–10/10–21	−0.07
P–O/P–O	D^*	21–17/20–16	−0.16
	D''	21–17/21–10	0.09
	D'	21–10/21–34	0.12
	D^0	21–10/20–35	−0.14

[a] Units: stretching and stretching/stretching in N · cm^{-1}, bending and torsion in N · cm · rad^{-2}.

In the refinement calculations of the force field, the Raman frequencies have been given particular attention for two reasons: the existence of Raman polarized spectra and the fact that the absorption bands observed on the ir spectra are due to the *LO* and *TO* modes so that values of the *TO* frequencies are not accurately known. The high frequencies assigned to P–O and Sb–O stretching vibrations where the coupling effects are weak have been refined first; then, the lower frequencies have been adjusted.

Table III compares the observed and calculated frequencies and gives the potential energy distribution (PED) for $K_3Sb_3P_2O_{14},xH_2O$. It can be seen that, with regard to the assignment of the A_{1g} and E_g modes inferred from the polarized spectra, the line at 599 cm^{-1} has been incorporated as an E_g line and the 179 cm^{-1} shoulder has been considered to be a splitting of the 158 cm^{-1} line. This result is supported by the fact that a 600 cm^{-1} frequency exists in the four active modes. The examination of Table III points out the following results:

—From 1400 to 900 cm^{-1} the P–O stretching vibrations are practically pure.

—From 780 to 750 cm^{-1} two modes correspond to the symmetric (E_g) and the antisymmetric (E_u) d_1 stretching modes.

—At about 600 cm^{-1} four modes are due to a coupling between d_2 stretching and O–P–O and Sb–O–P bending vibrations.

—From 520 to 450 cm^{-1} four modes involve only deformations of the octahedra in the SbO_6 network.

—Below 450 cm^{-1}, very strong couplings result essentially from bending modes. They correspond to deformations of the polyhedra but also of the whole covalent network; two frequencies are noticeable:

- the A_{1g} mode at 339 cm^{-1} which is practically pure on the O–Sb–O bending vibrations;
- the A_{1g} mode at 307 cm^{-1} which is due to d_2 bond and β angle motions. The vibra-

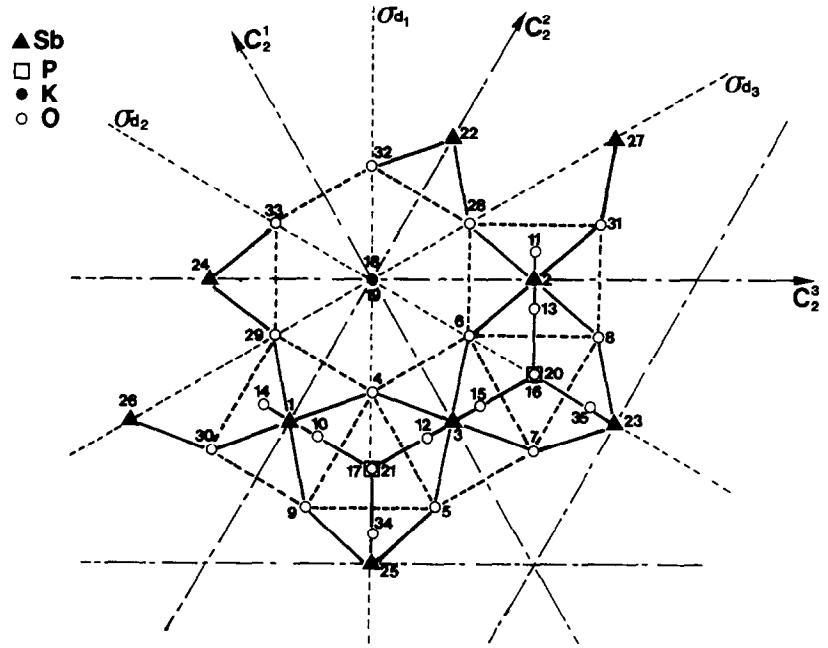

FIG. 5. Projection of the structure of $K_3Sb_3P_2O_{14},xH_2O$ on the (001) plane with numbered atoms.

tion scheme of this mode calculated by the program shows a sort of "breathing" mode of the covalent layer along the [001] direction; the motion of each PO_4 group in this direction involving that of the associated d_2 bonds.

—Below 150 cm^{-1} four modes due to the K–O ionic bonds are found; the four others, predicted by the theoretical numbering of vibrations, concern the K–O bonds of 2.95 Å, not introduced in the calculations. These appear certainly at very low frequencies ($\leq$80 cm^{-1}).

The calculated force constants are reported in Table II. The P–O terminal bonds have a force constant about 28% higher than that of the P–O bridged bonds in agreement with the difference of chemical environment. For the Sb–O bonds, d_1 bonds have a range of frequencies and a force constant very close to those found for antimonates of pyrochlore structure presenting the same type of bonds (*14*). The d_2 bonds have a lower range of frequencies and a force constant about 12% weaker than the d_1 bonds: their oxygen atom is strongly bonded to a phosphorous atom and so d_2 bonds are weakened. The f(O–Sb–O) and f(O–P–O) bending constants have values coherent with the corresponding stretching constants. On the other hand, f(Sb–O–P) is relatively high thus confirming the strong interactions existing between the SbO_6 and PO_4 polyhedra. On the contrary, the Sb–O–Sb bending and the O–Sb–O–Sb torsion play a negligible role and their force constants have been cancelled in the last cycles of refinement. In the same way, all the stretching/stretching interactions have been incorporated but only the most significant were retained. Among them, the D^0 and D^* interactions are interesting: they concern two P–O bonds belonging to two different PO_4 groups joined via an antimony atom. This type of coupling has already been pointed out for the 307 cm^{-1} Raman active mode.

TABLE III

OBSERVED AND CALCULATED FREQUENCIES AND PED IN $K_3Sb_3P_2O_{14},xH_2O$

Obs. freq.		Calc. freq.				
Raman	ir	A_{1g}	E_g	A_{2u}	E_u	PED (%)
	1284 1255			1252.9		$77D_1 + 16D_2$
1211		1231.8				$78D_1 + 17D_2$
	1190				1152.4	$88D_2$
1095			1135.9			$91D_2$
984		953.2				$61D_2 + 19D_1 + 14d_2$
	970 955			960.2		$61D_2 + 17D_1 + 15d_2$
777			769.8			$90d_1$
	780 755				768.3	$100d_1$
601		598.3				$23d_2 + 27\beta + 25\delta + 14\gamma$
	600			598.2		$33d_2 + 25\beta + 25\delta$
					609.5	$66d_2 + 23\beta + 13\delta$
599			608.4			$50d_2 + 26\beta + 15\delta$
	517				504.9	$66d_1 + 21\gamma + 11\Delta$
	490			483.7		$66d_1 + 19\gamma + 10\Delta$
485.5		488.5				$35d_1 + 36\gamma + 15\Delta$
468			474.9			$24d_1 + 42\gamma + 21\beta$
	406				412.9	$67\beta_1 + 22\gamma$
377			379.0			$43\beta_1 + 28d_1 + 14\Delta$
	n.o.[a]			358.7		$45d_2 + 19\gamma + 18\beta + 11\delta$
339		334.7				83γ
307		291.7				$51d_2 + 25\beta$
	298			307.7		$78\gamma + 11\Delta$
					309.2	$86\gamma + 12\beta_2$
268			262.3			$40\beta + 28\gamma + 16\delta$
	263				268.6	$48\beta + 33\gamma$
	250				236.7	$21d_{1,2} + 46\gamma + 20\delta$
	233			230.7		$26d_{1,2} + 57\gamma + 13\beta$
216			222.9			$52\gamma + 37\beta$
	n.o.				205.9	$17d_{1,2} + 35\gamma + 37\Delta$
179 158			154.4			$20d_2 + 46\gamma + 14\beta$
n.o.			114.4			$16d_1 + 68\Delta$
	n.o.				110.5	83γ
	n.o.				107.4	$49\gamma + 44\Delta$
84		78.0				85Δ
	n.o.		77.8	77.8		$21\gamma + 74\Delta$

Note. Only the contributions $\geq 10\%$ are mentioned.

[a] n.o., no observation.

The vibrational analysis has been made without considering the H_2O molecules located in the interlayer space. One can assume that their oxygen atoms are bonded to K^+ cations and their hydrogen atoms establish hydrogen bonding with the oxygen atoms of the D_2 P–O bonds. These molecules have little influence on the covalent net-

work. The ir band observed at 3520 cm^{-1} in Fig. 3 is characteristic of a weakly bonded water; however, the water molecules may be responsible for the splitting observed for some vibrations: 1284–1255, 995–984, and 970–955 according to whether the oxygen atom of the D_2 bonds is hydrogen bonded or not. In the same way, the fact that the potassium sites are not fully occupied could also explain the splitting of some bands, especially those involving the d_1 bonds which may or not share their oxygen atom with a K^+ cation; this is the case, for example, for the 780- to 755-cm^{-1} ir band.

Conclusion

This study allows precise assignment of all the frequencies in Raman spectroscopy and also calculation of a force field, the validity of which is then checked by the calculation of active ir absorption frequencies. The valence force field is defined with nine force and eight interaction constants. The average difference between calculated and experimental frequencies is about 2.2%. This fair agreement justifies the choice of a simplified model of structure for the calculations. This work is part of a complete characterization (structural and spectroscopic) of materials, the properties of which are now being studied.

References

1. Y. Piffard, A. Lachgar, and M. Tournoux, *J. Solid State Chem.* **58,** 253 (1985).
2. A. Lachgar, S. Deniard-Courant, and Y. Piffard, *J. Solid State Chem.* **73,** 572 (1988).
3. Y. Piffard, A. Verbaere, A. Lachgar, S. Deniard-Courant, and M. Tournoux, *Rev. Chim. Miner.* **23,** 766 (1986).
4. S. Deniard-Courant, Y. Pifford, Ph. Barboux, and J. Livage, *Solid State Ionics*, submitted.
5. J. H. Schachtschneider, Shell Development Co., Technical Report 231-264, 57–65 (1964).
6. J. B. Bates, *J. Chem. Phys.* **56,** 1910 (1972).
7. T. Shimanouchi, M. Tsuboï, and T. Miyazawa, *J. Chem. Phys.* **35,** 1597 (1961).
8. R. D. Shannon and C. T. Prewitt, *Acta Crystallogr. Sect. B* **25,** 925 (1969).
9. S. Bhagavantam and T. Venkataryudu, *Proc. Indian Acad. Sci. A* **9,** 224(1939).
10. R. S. Halford, *J. Chem. Phys.* **14,** 1 (1946).
11. K. Nakamoto, "Infrared and Raman Spectra of Inorganic and Coordination Compounds," Wiley, New York (1978).
12. S. P. S. Porto and J. F. Scott, *Phys. Rev.* **157,** 716 (1967).
13. A. Lachgar, Thesis, Nantes University (1987).
14. M. T. Vandenborre, E. Husson, and J. L. Fourquet, *Spectrochim. Acta Part A* **38,** 997 (1982).